On the Modeling and Control of Coupled Multi-Loop Thermosyphons

YAN WU
Department of Mathematical Sciences
Georgia Southern University
Statesboro, GA 30460
USA
yan@georgiasouthern.edu

Abstract: - This paper presents a one-dimensional model for natural convection in coupled multi-loop thermosyphons. The physical model is governed by a system of Navier-Stokes equations, which are reduced to coupled systems of Lorenz equations via the Galerkin method. The simulations reveal different stages of flow as the Rayleigh number increases, e.g., from heat conduction, steady convective flow, to chaotic time-dependent flow. The control objective is to either stabilize the flow in each loop at one of its equilibrium points or track a reference signal in the chaotic range of the Rayleigh number. The controller design is based on proportional and integral (PI) control principles. The design can be easily implemented because the feedback state is measurable.

Key-Words: Thermosyphon; Navier-Stokes Equations; Lorenz equations; Proportional-integral control; Perturbation; Jacobian; Chaos

Mathematical Subject Classification: 93C15, 93C40, and 93C73

1 Introduction

New advances in the field of semiconductor electronics lead to significant increase in the number of micro-devices over a tiny area. The heat flux emitting from these devices also increased significantly. It is imperative that new technology for efficient thermal management be developed to dissipate high heat fluxes and maintain a working temperature for the microchips. Direct liquid cooling, i.e., the electronics are directly immersed in cool liquid, has been investigated extensively in [1-3] with some advantages and some shortcomings. Indirect liquid cooling using thermosyphons has been developed for thermal management [4]. Palm and Tengblad give a thorough review for the state-of-the-art technologies for cooling electronic devices with heat pipes and thermosyphons in [5]. Thermosyphons also have extensive applications in the cooling system of nuclear plants, railway track deicing, etc. Thermosyphon may come in different forms. In this paper, we study multi-loop thermosyphon systems whose geometry configuration is depicted in Fig.1. We consider two or more circular loops filled with incompressible fluid, The lower semicircles of the loops are heated with the heat index measured by the Rayleigh number, to be introduced later, while the upper portion of the loops are cooled through jackets surrounding the tubes filled with cold water. At a fixed point, $\varphi = \varphi_0$, we allow the fluids of the loops to be in direct contact. With these assumptions, the heat and momentum fluxes are established, driven by the local differences between the individual temperatures and velocities in the loops. By increasing the heat applied to the bottom of the loop(s) beyond certain threshold value, the initial state of heat conduction is replaced by a convective flow in either the clockwise direction or counter clockwise direction. By further increasing the imposed heat well above the critical value, the steady-state convective flow becomes unstable and will be replaced by a time-dependent flow, i.e., periodic doubling and chaos.

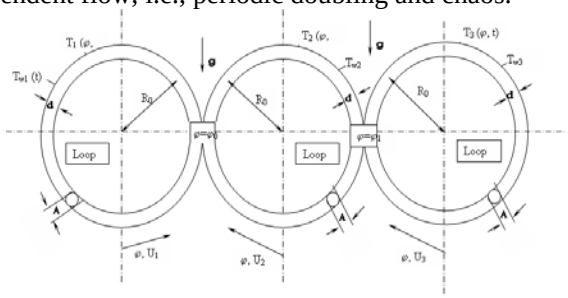

Fig. 1 Multi-loop thermosyphon

The control objective of this paper is in two-fold: given the parameter range in Rayleigh number that leads to chaotic flows in the loops, our goal is to perturb the Rayleigh number so that the flow is stabilized as a unidirectional convective flow under

high heat index; with the same setting, the other control objective is that the flow is driven to track a prescribed flow pattern. Our controller design is based on the principles of proportional and integral control with a measurable state variable, for the sake of implementation purpose. The governing equations for the multi-loop thermosyphons, as seen in the modeling section, are coupled Lorenz equations, which is a well-known nonlinear and chaotic system. This type of system can also be characterized as interconnected systems. Various decentralized controllers have been developed for nonlinear interconnected systems [6-7]. In [8], the design of the controller and the observer is formulated under the norm of linear matrix inequalities. Many decentralized control schemes developed for large-scale interconnected dynamical systems are multifaceted. They may not be implemental due to various restrictions. The implementation of linear controllers, however, is straightforward and cost effective. That is why they are most widely used controllers in modern industry, such as the PID controllers. This is the main motivation for this work, designing PI controllers to stabilize chaotic multi-loop thermosyphons. The rest of this paper is organized as follows: derivation of the modeling equations for the multi-loop thermosyphon is presented in section 2 with simulation results. In section 3, PI controllers are designed to stabilize the system at its equilibrium point or tracking an input signal. A local stability analysis is performed along with numerical simulations. Some remarks and future work are given in the conclusion section.

2 Modeling the thermosyphons

Natural convection in closed loops plays an important role on the design of thermal energy systems. These systems are characterized by at least one heat source and some heat sinks positioned at some height above the heat source. We consider N identical circular loops filled with incompressible fluids. The cross sections of the loops are circular and of constant area. We assume the fluids in the loops to be in direct contact at a fixed point $\varphi = \varphi_0$. The temperature distribution imposed on the tube walls are labeled as $T_{w_i}(\varphi)$. Under these conditions, heat and momentum fluxes are established, forced by the local differences between the individual temperatures and velocities in the loops.

It is sufficient to derive the differential equations for a three-loop system, see Fig. 1, and then generalize the model to an N-loop system. Assume the diameters of the cross section of the loop to be much smaller than its length, hence, a one-dimensional modeling of the flow and heat transfer process proves to be of sufficient accuracy [9]. Using the Boussinesq approximation, we obtain for the cross-sectionally averaged velocities $u_i(t)$ and the temperature $T_i(\varphi,t)$ in the loops the following set of partial differential equations:

$$\begin{cases} \rho_0 \dfrac{\partial u_1}{\partial t} = -\dfrac{\partial p_1}{R_0 \partial \varphi} - \rho(T_1) g \sin\varphi - f_{w_1} - \delta(\varphi-\varphi_0) f_{12} \\ \dfrac{\partial u_1}{R_0 \partial \varphi} = 0 \\ \rho_0 c_p \left(\dfrac{\partial T_1}{\partial t} + \dfrac{u_1}{R_0} \dfrac{\partial T_1}{\partial \varphi} \right) = h_w \left(T_{w_1}(\varphi) - T_1 \right) + \delta(\varphi-\varphi_0) h_{12} (T_2 - T_1) \end{cases} \tag{1}$$

$$\begin{cases} \rho_0 \dfrac{\partial u_2}{\partial t} = -\dfrac{\partial p_2}{R_0 \partial \varphi} - \rho(T_2) g \sin\varphi - f_{w_2} - \delta(\varphi-\varphi_0) f_{21} \\ \qquad - \delta(\varphi-\varphi_1) f_{23} \\ \dfrac{\partial u_2}{R_0 \partial \varphi} = 0 \\ \rho_0 c_p \left(\dfrac{\partial T_2}{\partial t} + \dfrac{u_2}{R_0} \dfrac{\partial T_2}{\partial \varphi} \right) = h_w \left(T_{w_2}(\varphi) - T_2 \right) + \delta(\varphi-\varphi_0) h_{21} (T_1 - T_2) \\ \qquad + \delta(\varphi-\varphi_1) h_{23} (T_3 - T_2) \end{cases}$$

$$\begin{cases} \rho_0 \dfrac{\partial u_3}{\partial t} = -\dfrac{\partial p_3}{R_0 \partial \varphi} - \rho(T_3) g \sin\varphi - f_{w_3} - \delta(\varphi-\varphi_1) f_{32} \\ \dfrac{\partial u_3}{R_0 \partial \varphi} = 0 \\ \rho_0 c_p \left(\dfrac{\partial T_3}{\partial t} + \dfrac{u_3}{R_0} \dfrac{\partial T_3}{\partial \varphi} \right) = h_w \left(T_{w_3}(\varphi) - T_3 \right) + \delta(\varphi-\varphi_1) h_{32} (T_2 - T_3) \end{cases}$$

where $u_i(t)$ is the average velocity of fluid flow in loop i, p_i is total pressure in loop i, T_i is cross-sectionally averaged temperature distribution in loop i, ρ_0 and $\rho(T_i)$ are average density of fluid and density of fluid, respective, f_{ij} represents friction force due to shear flow from loop i to loop j, h_w is heat transfer coefficient at the wall, f_{w_i} is friction force at wall in loop i, and finally h_{ij} is coefficient of heat transfer from loop i to loop j. In the laminar flow regime, it is convenient to use the linear correlation between the friction force f_{w_i} and the velocity u_i, i.e. $f_{w_i} = \frac{\rho_0}{2} f_{w_0} u_i$. The friction force at the contact surface is also approximated by $f_{ij} = \frac{\rho_0}{2} K_M f_{w_0} (u_i - u_j)$, where K_M is the coupling intensity of the momentum. Similarly, the coefficient of heat transfer is approximated by a linear correlation $h_{ij} = K_H h_w$, where K_H is the coupling intensity of heat, which is known to be a good

approximation for the inter-fluid heat exchange. Notice that the temperature distribution $T_i(\varphi,t)$ is periodic in φ. We apply Fourier series expansion on T_i,

$$T_i(\varphi,t)=T_{i0}+\sum_{n=1}^{\infty}[S_{i,n}(t)\sin(n\varphi)+C_{i,n}(t)\cos(n\varphi)] \quad (2)$$

Based on the Boussinesq approximation, we assume that all fluid properties are independent of temperature with the exception that the fluid density varies linearly as follows,

$$\rho(T_i)=\rho_0(1-\alpha_0(T_i-T_0)) \quad (3)$$

where α_0 is the thermal expansion coefficient. We proceed to non-dimensionalize the state variables and time as follows,

$$\begin{aligned} t'&=\frac{h_w}{\rho_0 c_p}t, & x_1&=\frac{\rho_0 c_p}{h_w R_0}u_i \\ x_2&=\frac{\rho_0 c_p \alpha_0 g}{h_w R_0 f_{w_0}}S_{11}, & x_3&=\frac{\rho_0 c_p \alpha_0 g}{h_w R_0 f_{w_0}}(\Delta T-C_{11}) \\ y_1&=\frac{\rho_0 c_p}{h_w R_0}u_2, & y_2&=\frac{\rho_0 c_p \alpha_0 g}{h_w R_0 f_{w_0}}S_{21} \\ y_3&=\frac{\rho_0 c_p \alpha_0 g}{h_w R_0 f_{w_0}}(\Delta T-C_{21}) \end{aligned} \quad (4)$$

where ΔT measures the imposed temperature difference. And, x_1, y_1 represent the fluid velocity in loop 1 and loop 2, respectively; x_2, y_2 give measures for the horizontal temperature difference in each loop, while x_3, y_3 correspond to the vertical temperature difference in the loops. We initialize the coupling position at $\varphi_0=0$. We only listed the non-dimensionalization formulae for the state variables of the first two loops because the existing symmetry between the first loop and the third loop. Consider the momentum equation for loop 1 in (1), since $\frac{\partial u_1}{\partial t}=\frac{h_w^2 R_0}{(\rho_0 c_p)^2}\dot{x}_1$ (derivative with respect to t'), the momentum equation is non-dimensionalized as

$$\begin{aligned} \frac{h_w^2 R_0}{\rho_0 c_p^2}\dot{x}_1=\alpha_0\rho_0 g(T_1-T_0)\sin\varphi-\frac{1}{2}f_{w_0}\frac{h_w R_0}{c_p}x_1- \\ \delta(\varphi-\varphi_0)\frac{1}{2}K_M f_{w_0}\frac{h_w R_0}{c_p}(x_1-y_1) \end{aligned} \quad (5)$$

Now, integrate both sides of (5) with respect to φ around the loop, using Galerkin method to truncate (2) by only keeping the first-order terms, one has

$$\begin{aligned} \frac{2\pi h_w^2 R_0}{\rho_0 c_p^2}\dot{x}_1=\pi\alpha_0\rho_0 g S_{11}-\frac{\pi f_{w_0} h_w R_0}{c_p}x_1- \\ \frac{1}{2}K_M f_{w_0}\frac{h_w R_0}{c_p}(x_1-y_1) \end{aligned} \quad (6)$$

With the help of (4), Eqn (6) is further simplified as

$$P^{-1}\dot{x}_1=x_2-x_1-\gamma(x_1-y_1) \quad (7)$$

where $P=\frac{f_{w_0}\rho_0 c_p}{2h_w}$, which is comparable to the Prandtl number in ordinary viscous fluid flow and depends only on the properties of the fluid and the wall material, and $\gamma=\frac{K_M}{2\pi}$.

Our next step is to simplify the energy equation in (1). Using Galerkin method on the Fourier series expansion of T_i given by (2), the left side of the energy equation can be written as, after non-dimensionalization,

$$\begin{aligned} &\rho_0 c_p\left(\frac{\partial T_1}{\partial t}+\frac{u_1}{R_0}\frac{\partial T}{\partial\varphi}\right)= \\ &\frac{h_w^2 R_0 f_{w_0}}{\rho_0 c_p\alpha_0 g}\left(\dot{x}_2+(x_3-\frac{\rho_0 c_p\alpha_0 g}{h_w R_0 f_{w_0}}\Delta T)x_1\right)\sin\varphi+ \\ &\frac{h_w^2 R_0 f_{w_0}}{\rho_0 c_p\alpha_0 g}(-\dot{x}_3+x_1x_2)\cos\varphi \end{aligned} \quad (8)$$

The right side of the energy equation becomes

$$\begin{aligned} &h_w(T_{w_1}(\varphi)-T_1)+\delta(\varphi-\varphi_0)h_{12}(T_2-T_1)= \\ &h_w((\Delta T-C_{11})\cos\varphi-S_{11}\sin\varphi)+ \\ &\delta(\varphi-\varphi_0)K_H h_w^2((C_{21}-C_{11})\cos\varphi+(S_{21}-S_{11})\sin\varphi) \\ &=\frac{h_w^2 R_0 f_{w_0}}{\rho_0 c_p\alpha_0 g}(x_3\cos\varphi-x_2\sin\varphi)+ \\ &\delta(\varphi-\varphi_0)\frac{h_w^2 R_0 f_{w_0}K_H}{\rho_0 c_p\alpha_0 g}(x_3-y_3)\cos\varphi \end{aligned} \quad (9)$$

By comparing (8) and (9) in $\sin\varphi$ and $\cos\varphi$, respectively, one obtains the following equations:

$$\begin{aligned} \dot{x}_2&=R_1x_1-x_1x_3-x_2 \\ \dot{x}_3&=x_1x_2-x_3-K_H(x_3-y_3) \end{aligned} \quad (10)$$

where $R_1=\frac{\rho_0 c_p\alpha_0 g}{h_w R_0 f_{w_0}}\Delta T$, which is analogous to the Rayleigh number. Rayleigh number measures the level of external heat applied to the thermal loop. We thus obtained the system of ODEs for the first loop combining (7) and (10), which are similar to the

ISBN: 978-960-474-270-7

Lorenz equations. The governing equations for the middle loop as well as the end loop are derived in a similar fashion. Note that there are two coupling points for the middle loop. For the sake of argument, from this point on, we redefine the state variables $\{u_i, x_i, y_i\}$ as velocity and temperature coefficients for loop *i*. Therefore, the system of differential equations for N-loop thermosyphons is given as follows,

$$\text{Loop 1: } \begin{cases} \dot{u}_1 = P(x_1 - u_1 - \gamma(u_1 - u_2)) \\ \dot{x}_1 = R_1 u_1 - u_1 y_1 - x_1 \\ \dot{y}_1 = u_1 x_1 - y_1 - L(y_1 - y_2) \end{cases}$$

Loop *k*:

$$\begin{cases} \dot{u}_k = P(x_k - u_k - \gamma(u_k - u_{k-1}) - \gamma(u_k - u_{k+1})) \\ \dot{x}_k = R_k u_k - u_k y_k - x_k \\ \dot{y}_k = u_k x_k - y_k - L(y_k - y_{k-1}) - L(y_k - y_{k+1}) \end{cases}$$
$$k = 2,3,...,N-1$$

$$\text{Loop } N\text{: } \begin{cases} \dot{u}_N = P(x_N - u_N - \gamma(u_N - u_{N-1})) \\ \dot{x}_N = R_N u_N - u_N y_N - x_N \\ \dot{y}_N = u_N x_N - y_N - L(y_N - y_{N-1}) \end{cases} \qquad (11)$$

It is reasonable to assume that all the coupling coefficients, γ, L, are identical as well as the Prandtl number among the loops. It is also widely accepted that the Prandtl number is set to be 10. In the numerical simulations, we set the coupling coefficients equal to unity. Of course, the greater values for γ, L, the higher intensity in coupling, which could be exploited in controller designs. According to [10], these coupling coefficients are indeed of order 1. The dynamical system is solved numerically via the 4th order Runge-Kutta method. In general, as the Rayleigh number increases, we observe heat conduction, co-current and counter-current steady flow and irregular time-dependent flows. It is important to point out that chaotic flows are observed when the Rayleigh numbers R_k's are over 28.

3 Controlling the thermosyphons

In this work, we are interested in stabilizing flows in the interconnected chaotic thermosyphon loops via classical control methodology to achieve good stability and tracking properties under chaos, i.e. the Rayleigh numbers are greater than 28. Since the three loop setting, Fig.1, truly represents the dynamical structure of any number of loops greater than three, we only consider the controller design for the three-loop systems in this paper. Even with three loops, there are a number of possible configurations for controlling the system. Due to the existing similarities among the configurations, we will focus on a local control scheme, i.e. the actuator is implemented with the middle loop as a perturbation to the Rayleigh number R_2. This is also known as a single-input-single-output (SISO) control system. Of course, more than one control input can be implemented. For example, there is a controller for each loop, which leads to multi-input-multi-output (MIMO) control systems. Our experiment shows that the proposed SISO control is sufficient to stabilize the flow in all loops. We apply small perturbations to stabilize the flow at one of the system's equilibria. Large perturbations are explored to make system track an input signal (a prescribed convective flow pattern).

To set the stage, consider $N = 3$ in (11). Let X_{ss} be the steady state or the equilibrium of the 9-dimensional system, i.e. $X_{ss} = \{\bar{u}_i, \bar{x}_i, \bar{y}_i\}_{i=1,2,3}$. The steady state is found by setting the derivatives equal to zero. However, there is no closed-form formula for the equilibrium. One has to take resort to numerical methods for solving the nonlinear algebraic equations. We are able to find the I/O representation from linearizing the system at the equilibrium point. The state space form of the I/O representation is given by $\{A, B, C\}$. The state matrix *A* is also known as the Jacobian matrix associated with the system. The input structure matrix *B* is known as the input Jacobian. We choose the output matrix *C* as follows,

$$C = [0 \quad 0 \quad 0 \quad 0 \quad 1 \quad 0 \quad 0 \quad 0 \quad 0] \qquad (12)$$

This is because the state variable x_2 corresponds to the vertical temperature difference across loop 2, which can be easily measured.

Now, with a small perturbation to R_2, the control system is given by

$$\begin{cases} \dot{u}_1 = P(x_1 - u_1 - \gamma(u_1 - u_2)) \\ \dot{x}_1 = R_1 u_1 - u_1 y_1 - x_1 \\ \dot{y}_1 = u_1 x_1 - y_1 - L(y_1 - y_2) \end{cases}$$

$$\begin{cases} \dot{u}_2 = P(x_2 - u_2 - \gamma(u_2 - u_1) - \gamma(u_2 - u_3)) \\ \dot{x}_2 = (R_2 + v)u_2 - u_2 y_2 - x_2 \\ \dot{y}_2 = u_2 x_2 - y_2 - L(y_2 - y_1) - L(y_2 - y_3) \end{cases}$$

ISBN: 978-960-474-270-7

$$\begin{cases} \dot{u}_3 = P(x_3 - u_3 - \gamma(u_3 - u_2)) \\ \dot{x}_3 = R_3 u_3 - u_3 y_3 - x_3 \\ \dot{y}_3 = u_3 x_3 - y_3 - L(y_3 - y_2) \end{cases} \tag{13}$$

It is understood that, from the output feedback design point of view, the small perturbation ν is proportional to the perturbation (as a state variable in the linearized system) of x_2. We first obtain the Jacobian matrix with respect to $X_{ss} = \{\bar{u}_i, \bar{x}_i, \bar{y}_i\}_{i=1,2,3}$ as follows,

$$A = \begin{bmatrix} -P(1+\gamma) & P & 0 & \gamma P & 0 & 0 & 0 & 0 & 0 \\ R_1 - \bar{y}_1 & -1 & -\bar{u}_1 & 0 & 0 & 0 & 0 & 0 & 0 \\ \bar{x}_1 & \bar{u}_1 & -1-L & 0 & 0 & L & 0 & 0 & 0 \\ \gamma P & 0 & 0 & -P(1+2\gamma) & P & 0 & \gamma P & 0 & 0 \\ 0 & 0 & 0 & R_2 - \bar{y}_2 & -1 & -\bar{u}_2 & 0 & 0 & 0 \\ 0 & 0 & L & \bar{x}_2 & \bar{u}_2 & -1-2L & 0 & 0 & L \\ 0 & 0 & 0 & \gamma P & 0 & 0 & -P(1+\gamma) & P & 0 \\ 0 & 0 & 0 & 0 & 0 & 0 & R_3 - \bar{y}_3 & -1 & -\bar{u}_3 \\ 0 & 0 & 0 & 0 & 0 & L & \bar{x}_3 & \bar{u}_3 & -1-L \end{bmatrix} \tag{14}$$

and the input Jacobian matrix

$$B = [0 \quad 0 \quad 0 \quad 0 \quad \bar{u}_2 \quad 0 \quad 0 \quad 0 \quad 0]^T \tag{15}$$

The corresponding transfer function is in the form of

$$H(s) = \frac{b_1 s^8 + b_2 s^7 + \ldots + b_8 s + b_9}{s^9 + a_1 s^8 + \ldots + a_8 s + a_9} \tag{16}$$

Consider a proportional negative feedback, $\nu = -k\delta x_2$, the closed-loop transfer function is

$$\tilde{H}(s) = \frac{H(s)}{1 + kH(s)} \tag{17}$$

A root locus analysis for the closed-loop poles indicates that, as the gain *k* increases, the steady state becomes stable even if the gain approaches infinity, see Fig. 2. Recall that the controller is incorporated in the second loop only. By stabilizing the flow in the second loop, the flows in its adjacent loops are automatically stabilized. A time response is of (13) with a proportional controller is given in Fig. 3. The loop gain used in this simulation is 2.5.

We further studied the proportional-plus-integral (PI) controller design to test the tracking ability of system (13). The difference between this approach and the previous regulating problem is that the perturbation is proportional to the x_2-state instead of a small variation of x_2, as such it is called large perturbation. Since the PI control is a dynamical form of compensation, the original system is augmented to include integral dynamics of the tracking error. The new 10-state system is show below:

$$\begin{cases} \dot{u}_1 = P(x_1 - u_1 - \gamma(u_1 - u_2)) \\ \dot{x}_1 = R_1 u_1 - u_1 y_1 - x_1 \\ \dot{y}_1 = u_1 x_1 - y_1 - L(y_1 - y_2) \end{cases}$$

$$\begin{cases} \dot{u}_2 = P(x_2 - u_2 - \gamma(u_2 - u_1) - \gamma(u_2 - u_3)) \\ \dot{x}_2 = (R_2 - k(x_2 - x_f) - h\theta)u_2 - u_2 y_2 - x_2 \\ \dot{y}_2 = u_2 x_2 - y_2 - L(y_2 - y_1) - L(y_2 - y_3) \\ \dot{\theta} = x_2 - x_f \end{cases}$$

$$\begin{cases} \dot{u}_3 = P(x_3 - u_3 - \gamma(u_3 - u_2)) \\ \dot{x}_3 = R_3 u_3 - u_3 y_3 - x_3 \\ \dot{y}_3 = u_3 x_3 - y_3 - L(y_3 - y_2) \end{cases} \tag{18}$$

where $k > 0$ is the gain on proportional control and $h > 0$ is the gain on the integral controller. Again, the steady state of the extended control system (18) has to be found numerically. However, it is easy to see that $\bar{x}_2 = x_f$ as one of the coordinates of the equilibrium point. Linear stability test in this case is to simply locate the eigenvalues of the Jacobian matrix associated with (18) with the computed equilibrium. The root locus analysis shows that the system is stabilized at the equilibrium point with appropriate gains. A simulation for (18) is shown in Fig. 4. In the simulation, the reference signal x_f consists of two step inputs. The first step input equals $\bar{x}_2$, while the second step input is -10.2. The step responses show that the system is able to track the step inputs rather quickly.

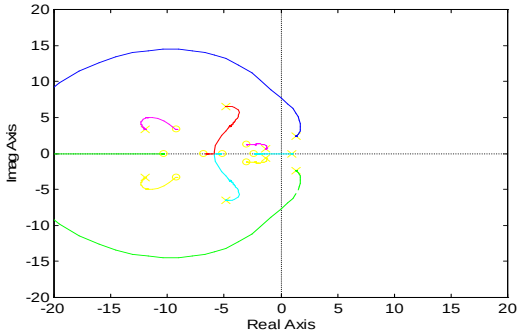

Fig. 2 Root locus of the close-loop poles for the x_2 feedback

ISBN: 978-960-474-270-7

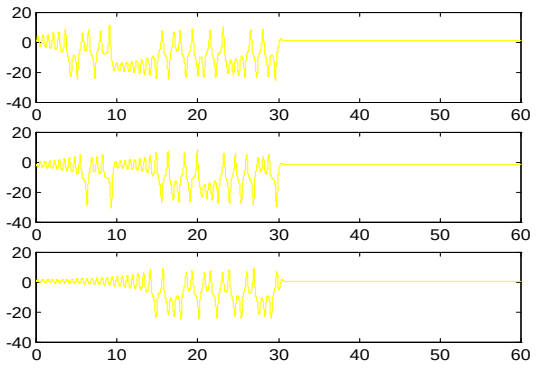

Fig.3 Time-response of the velocities in each of the three loops with the proportional control. The controller is activated at $t = 30s$.

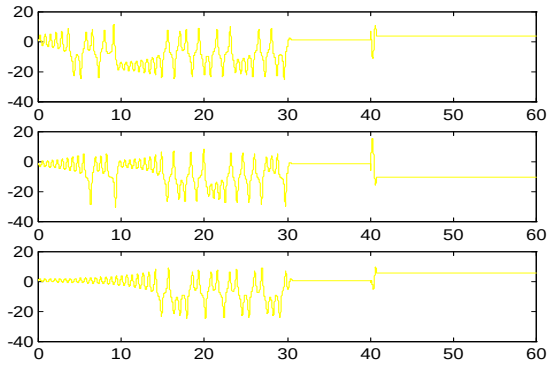

Fig. 4 Time-response of the *x*-state (temperature) in each of the three loops. PI controller for tracking step inputs while the system is in chaotic regime. The controller is activated at $t = 30s$. It is reactivated automatically when the step input changes.

4 Conclusion

In this paper, we present the modeling of high-dimensional multi-loop thermosyphon systems and its control perspectives. The governing equations are in essence coupled Lorenz equations. The system is chaotic when the Rayleigh numbers are greater than a threshold value. Two control mechanisms are used to either stabilize the flow or make the system track a prescribed flow/temperature pattern. A qualitative stability analysis is difficult due to the dimension of the system, including the added dimensions of the system parameters. However, the local perturbation approach is still plausible due to its implementation consideration. The proposed PI controller design does require the system known *a priori*. We will explore adaptive control schemes for large scale thermosyphon systems with unknown parameters. Since the coupling between the loops is considered weak, we are also investigating the option of decentralized control via neural networks or wavelet networks.

References:

[1]F. P. Incropera, Liquid immersion cooling of electronic components, *Heat Transfer in Electronic and Microelectronic Equipment*, 1990, 407-444.

[2]W. Nakayama and A. E. Bergles, Cooling of electronic equipment: past, present, and future, *Heat Transfer in Electronic and Microelectronic Equipment*, 1990, 3-39.

[3] A. Bar-Cohen, Thermal management of electronic components with dielectric liquids, *Int. J. JSME*, ser. B, v 36, no. 1, 1993, 1-25.

[4] C. Ramaswamy, Y. K. Joshi, W. Nakayama, and W. B. Johnson, Combined effects of sub-cooling and operating pressure on the performance of a two-chamber thermosyphon, *IEEE Trans.Compon. and Packag. Tech.*, v. 23. no. 1, 2000, 61-69.

[5] B. Palm and N. Tengblad, Cooling of electronics by heat pipes and thermosyphons-a review of methods and possibilities, Proc. 31st Nat. Heat Transfer Conf., v. 7, 1996, 97-108.

[6] P. A. Ioannou, Decentralized adaptive control of interconnected systems, *IEEE Trans. Autom. Control*, v. 31, no. 4, 1986, 291-298.

[7] J. T. Spooner and K. M. Passino, Decentralized adaptive control of nonlinear systems using radial basis neural networks, *IEEE Trans. Autom. Control*, v. 44, no. 11, 1999, 2050-2057.

[8] Y. Zhu and P. R. Pagilla, Decentralized output feedback control of a class of large-scale interconnected systems, *IMA J. Math. Control Info*., v 24, no. 1, 2006, 57-69.

[9] P. Welander, On the oscillatory instability of a differentially heated fluid loop, *J. Fliud Mechanics*, v. 29, 1967, 17-30.

[10] P. Ehrhard, Ch. Karcher, and U. Muller, Dynamical behavior of Natural convection in a double-loop system, *Exp. Heat Transfer*, v. 2, 1989, 13-26.